Constant-Pressure Molecular Dynamics Investigation of Cholesterol Effects in a Dipalmitoylphosphatidylcholine Bilayer

Kechuan Tu,* Michael L. Klein,# and Douglas J. Tobias§

*Department of Pharmaceutical Chemistry, University of California, San Francisco, California 94143-0446; #Center for Molecular Modeling, Department of Chemistry, University of Pennsylvania, Philadelphia, Pennsylvania 19104-6323; and §NIST Center for Neutron Research, National Institute of Standards and Technology, Gaithersburg, Maryland 20899-0001, and Department of Chemistry, University of California, Irvine, California 92697-2025 USA

ABSTRACT We report a 1.4-ns constant-pressure molecular dynamics simulation of cholesterol at 12.5 mol% in a dipalmitoylphosphatidylcholine (DPPC) bilayer at 50°C and compare the results to our previous simulation of a pure DPPC bilayer. The interlamellar spacing was increased by 2.5 Å in the cholesterol-containing bilayer, consistent with x-ray diffraction results, whereas the bilayer thickness was increased by only 1 Å. The bilayer/water interface was more abrupt because the lipid headgroups lie flatter to fill spaces left by the cholesterol molecules. This leads to less compensation by the lipid headgroups of the oriented water contribution to the membrane dipole potential and could explain the experimentally observed increase in the magnitude of the dipole potential by cholesterol. Our calculations suggested that 12.5 mol% cholesterol does not significantly affect the conformations and packing of the hydrocarbon chains and produces only a slight reduction in the empty free volume. However, cholesterol has a significant influence on the subnanosecond time scale lipid dynamics: the diffusion constant for the center-of-mass "rattling" motion was reduced by a factor of 3, and the reorientational motion of the methylene groups was slowed along the entire length of the hydrocarbon chains.

INTRODUCTION

Cholesterol is an essential, ubiquitous component of eukaryotic plasma membranes. From decades of physical studies, it is well known that cholesterol has many effects on the structure and dynamics of lipid bilayers. For example, among other things, cholesterol reduces order in gel phase bilayers and increases order in liquid crystal phase bilayers, thereby broadening or even eliminating the main bilayer phase transition. Moreover, it is well known that cholesterol modulates the mechanical and transport properties of membranes. For example, adding cholesterol to a lipid bilayer increases its bending elasticity (Méléard et al., 1997) and reduces its passive permeability to small molecules (Carruthers and Melchior, 1983; Xiang and Anderson, 1997). Recent experimental and theoretical progress in understanding cholesterol effects in membranes has been reviewed by McMullen and McElhaney (1996). One of their conclusions was that, despite a great deal of research, the molecular picture of cholesterol-phospholipid interactions is still incomplete.

Computer modeling has the potential to supply some of the missing details. In the last 5 or so years there has been tremendous progress in the development and application of atomistic computer simulations to the study of model membranes (Pastor, 1994; Tobias et al., 1997a). Of the dozens of membrane simulations reported to date, two recently addressed the effects of cholesterol on lipid bilayer structure. Robinson et al. (1995) reported a constant-volume MD simulation of cholesterol at 10 mol% in a dimyristoylphosphatidylcholine (DMPC) bilayer at 50°C. They carried out a relatively detailed analysis of the DMPC acyl chain conformations, but did not have available a control calculation on a pure DMPC bilayer for comparison. Gabdoulline et al. (1996) performed MD simulations of pure DMPC and 1:1 DMPC:cholesterol bilayers and attempted to generate liquid crystal phase bilayers by heating crystal configurations at constant pressure from −73°C to 52°C. However, the results of these calcuations should be viewed cautiously, because the area per lipid for the pure liquid crystal phase DMPC bilayer was ~50 Å^2, ~20% lower than the experimental value.

In the present paper we expand upon these initial investigations by reporting a 1.4-ns constant-temperature and pressure (NPT) MD simulation of a dipalmitoylphosphatidylcholine (DPPC) bilayer containing 12.5 mol% cholesterol (i.e., a DPPC:cholesterol ratio of 8:1) at 50°C. We have investigated a variety of effects of cholesterol at this concentration on bilayer structure and dynamics by comparing to our previous simulation of a pure DPPC bilayer under the same conditions of temperature and hydration (Tu et al., 1995b). In addition to examining the effects of cholesterol on the overall bilayer structure and DPPC hydrocarbon chain conformations, we have focused in some detail on cholesterol effects on the structure and electrical properties of the membrane/water interface, the packing of the hydrocarbon chains, and the subnanosecond time scale motions of whole lipid molecules as well as the dynamics of conformational rearrangements in the bilayer interior.

Received for publication 26 January 1998 and in final form 31 July 1998.

Address reprint requests to Dr. Michael L. Klein, Department of Chemistry, University of Pennsylvania, Philadelphia, PA 19104-6323. Tel.: 215-898-8571; Fax: 215-898-8296; E-mail: klein@lrsm.upenn.edu.

0006-3495/98/11/2147/10 $2.00

MATERIALS AND METHODS

The initial structure of the DPPC/cholesterol bilayer was constructed from a configuration taken from the end of our previous simulation of a fully hydrated liquid crystal phase bilayer at 50°C (Tu et al., 1995), which consisted of 64 DPPC and 1792 water molecules with an average area per lipid of 61.8 Å^2 and a lamellar repeat of 67.3 Å. Eight well-separated DPPC molecules (four per monolayer) were removed and replaced with cholesterol molecules, yielding a bilayer with 12.5 mol% cholesterol (8 cholesterol/64 lipids). The eight cholesterol molecules in the unit cell of the monohydrate crystal (Craven, 1979) were taken as the initial cholesterol structures, and these were placed such that their hydroxyl oxygen atoms were at the same depth in the bilayer as the average of the carbonyl oxygens of the DPPC molecules that they replaced.

The DPPC/cholesterol bilayer was equilibrated at constant volume for 200 ps at a constant temperature of 50°C. This was followed by a 1400-ps constant-pressure and -temperature simulation in a fully flexible simulation cell at zero pressure and 50°C. The details of the simulation algorithm are identical to those reported by Tu et al. (1995b).

We used the same all-atom force fields for DPPC (Tu et al., 1995a; Tobias et al., 1997b) and water (Berendsen et al., 1987) that we employed in our previous simulations of gel (Tu et al., 1996) and liquid crystal phase (Tu et al., 1995b) DPPC bilayers. As for the lipid acyl chains, the all-atom cholesterol potential (Tu, 1995) was based largely on Williams model IV potential for hydrocarbons (Williams, 1967). Parameters used in the cholesterol potential but not reported by Tobias et al. (1997b) or Tu et al. (1995a) have been tabulated by Tu (1995). The Ewald sum was used to calculate the electrostatic forces, and a long-range correction to the pressure was used to account for truncated van der Waals interactions (Allen and Tildesley, 1989).

To check the quality of the cholesterol potential, we carried out constant-pressure simulations on cholesterol and cholesteryl acetate crystals with fully flexible simulation cells. Although such crystal calculations are not the final word on the performance of a potential in membrane simulations, they should reveal serious deficiencies when they exist (Tu et al., 1995a). The crystal simulations were initiated from the published x-ray structures of anhydrous cholesterol (Shieh et al., 1981), cholesterol monohydrate (Craven, 1979), and cholesteryl acetate (Weber et al., 1991). The cholesterol calculation was performed on 48 molecules arranged in a $2a \times b \times 3c$ lattice at a constant temperature of 25°C, the monohydrate calculation on 72 cholesterol plus 72 water molecules in a $3a \times 3b \times c$ lattice at 25°C, and the acetate calculation on 64 molecules in a $2a \times 4b \times 2c$ lattice at −150°C. Each simulation consisted of 10-ps equilibration at constant volume, 10-ps equilibration at constant pressure, and at least 50-ps data collection at constant pressure. Although short compared to the bilayer simulations, these equilibration periods are significantly longer than the time needed to converge the crystal structures (Tu et al., 1995a).

RESULTS AND DISCUSSION

The average unit cell parameters (a, b, c, α, β, and γ) and densities (d) from the cholesterol, cholesterol monohydrate, and cholesterol acetate crystal simulations are tabulated in Table 1. Overall, the agreement with the x-ray diffraction results is excellent: most of the parameters are within 1% of the experimental results, and the largest deviations are less than 3%. In light of the fact that the cholesterol and cholesterol monohydrate crystals each have eight different molecules (plus eight waters in the monohydrate) per unit cell, the agreement with experiment is noteworthy.

The time evolution of the bilayer area and interlamellar spacing during the 1.4-ns constant NPT MD simulation of the DPPC/cholesterol bilayer at 50°C is shown in Fig. 1. These quantities drifted from their initial values until ~700 ps had elapsed, which we regard as equilibration and discard. During the last 700 ps, which we have used for all of the analysis reported below, the bilayer area and lamellar repeat appear to have settled into oscillations around stable average values of 1860 Å^2 and 69.8 Å, respectively. The former is 120 Å^2 less and the latter is 2.5 Å greater than the corresponding results from our previous simulation of a pure DPPC bilayer (Tu et al., 1995b), which was in excellent agreement with x-ray diffraction data on fully hydrated DPPC bilayers. The magnitude of the increase in interlamellar spacing upon the addition of 12.5 mol% cholesterol to the liquid crystal phase of DPPC is very close to that observed for a similar cholesterol concentration in DMPC by x-ray diffraction (Hui and He, 1983). The contraction of the bilayer area, caused primarily by the replacement of four DPPC molecules by the "skinnier" cholesterol molecules, is accompanied by an increase in the thickness of the water layer, so that the water density is not changed significantly. Despite the relatively large 4% increase in the lamellar spacing and 6% decrease in the bilayer area, there is only a 2% reduction in the volume of the DPPC/cholesterol system compared to the pure DPPC system. The smaller volume may be accounted for by a decrease in thickness of the of the DPPC/cholesterol bilayer (see below). A snapshot from the end of the MD simulation of the cholesterol containing DPPC bilayer is shown in Fig. 2 *a*. One can see from the figure that the cholesterol molecules were initially placed and remained well separated from one another. It is also evident that the cholesterol molecules are located at a range of depths within the bilayer, and their long axes are tilted significantly with respect to the bilayer normal. The average tilt, defined as the angle between the bilayer normal and the

TABLE 1 Comparison of x-ray and NPT MD results for the crystal unit cell parameters and densities of cholesterol, cholesterol monohydrate, and cholesteryl acetate crystals

Crystal		a (Å)	b (Å)	c (Å)	α (°)	β (°)	γ (°)	d (g/cm^3)
Cholesterol (25°C)	X-ray*	14.17	34.21	10.48	94.6	90.7	96.3	1.02
	MD	14.01	34.04	10.41	94.4	90.8	97.2	1.05
Cholesterol monohydrate	X-ray[#]	12.39	12.41	34.36	91.9	98.1	100.8	1.05
(25°C)	MD	12.51	12.07	34.52	89.5	99.4	100.5	1.06
Cholesterol acetate	X-ray[§]	16.54	9.29	17.64	90.0	106.9	90.0	1.10
(−150°C)	MD	16.55	9.30	17.50	90.0	107.0	90.0	1.11

*Shieh et al. (1981).
[#]Craven (1979).
[§]Weber et al. (1991).

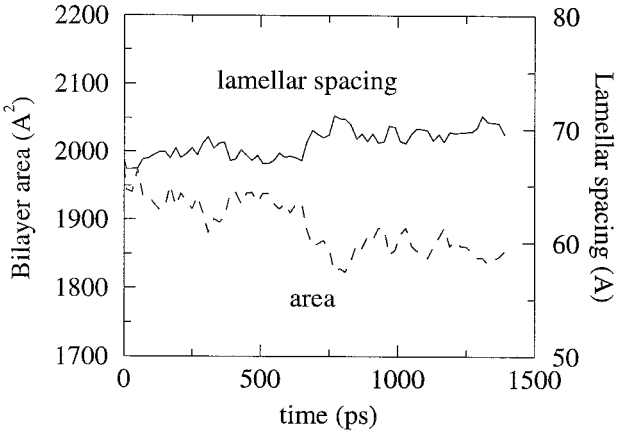

FIGURE 1 Time evolution of the bilayer area (28 DPPC plus 4 Chol) and lamellar spacing during the NPT MD simulation. These dimensional parameters appear to have converged after 700 ps.

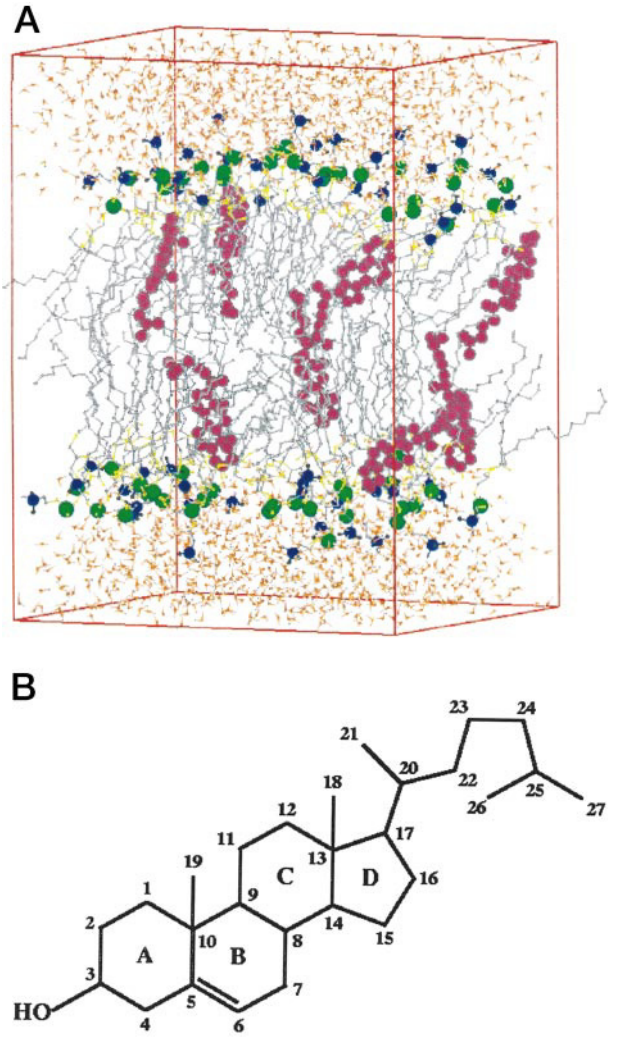

FIGURE 2 (*a*) Snapshot of a configuration from the MD simulation. The central simulation cell is outlined in red, and the lipid H atoms have been removed for viewing clarity. The coloring scheme is: water O, orange; cholesterol C, magenta; N, blue; P, green; C, gray; and lipid O, yellow. Note that the cholesterol molecules display an appreciable tilt with respect to the bilayer normal. (*b*) The molecular structure of cholesterol with the carbon atoms and rings labeled. The stereochemistry of cholesterol is such that the C18 and C19 methyl groups are both on the same (α) side of the approximately planar sterol ring system (the opposite side is referred to as the β side).

vector connecting the cholesterol C3 and C17 atoms (see Fig. 2 *b* for atom labels), is 14°, which is close to the range of values, 16° to 17° estimated from deuterium NMR measurements on cholesterol from 10 to 50 mol% in DMPC at 23°C (Oldfield et al., 1978).

The rigid sterol nucleus and short, flexible 17β hydrocarbon tail in cholesterol and related molecules plays an important role in determining the conformations of neighboring molecules in the lipid matrix. Steroids that have saturated nuclei are essentially inflexible, whereas cholesterol, with its unsaturated carbon-carbon bond in the 5-ene B ring, does display multiple sterol ring conformations in crystals. To see the extent to which the situation may be different in bilayers, we have analyzed the structures of the cholesterol molecules in our simulation and compared them to x-ray crystal structures. The conformations of the B rings generally range about the symmetrical 8β, 9α half-chair conformation in which atoms C10, C5, C6, and C7 are coplanar because of the C5-C6 double bond, and C8 and C9 are displaced on the β and α sides, respectively, of the plane (see Fig. 2 *b*). If C8 or C9 becomes coplanar with C10, C5, C6, and C7, the B ring has the 9α sofa or 8β sofa conformation, respectively. In our simulation the B ring exhibited considerable flexibility, but preferred the 8β, 9α half-chair conformation to both the 8β sofa and 9α sofa conformations. In the cholesterol monohydrate crystal the preferred conformations are between the 8β, 9α half-chair and 9α sofa conformations, whereas in the cholesterol acetate crystal one molecule in the unit cell prefers the 9α sofa and the other the 8β sofa conformation. To characterize the conformational disorder in the hydrocarbon tail, we calculated the average fraction *gauche* conformations, obtaining for the last five bonds 0.04 (C17-C20), 0.21 (C20-C22), 0.11 (C22-C23), 0.22 (C23-C24), and 0.50 (C24-C25). From a survey of 96 crystallographically independent examples of the conformation of the cholestane side chain, Rohrer et al. (1980) concluded that there are four primary conformers: the fully extended chain (A), and three conformers (B, C, and D) distinguished by *gauche* defects in the C23-C24, C22-C23, and C20-C22 bonds, respectively. The probabilities of occurrence of conformations A, B, C, D in the 96 examples are 0.72, 0.08, 0.08, and 0.11, respectively. In our simulation the relative populations were 0.55, 0.12, 0.11, and 0.12, whereas in the monohydrate crystal four of the eight molecules in the unit cell are B and four are C, and in the acetate crystal both molecules in the unit cell are A.

For the purpose of discussing the effects of cholesterol at 12.5 mol% on the overall structure of the bilayer, in Fig. 3 *a* we compare the electron density profiles as a function of distance along the bilayer normal computed as decribed by Tu et al. (1995b) from the two simulations. The basic form

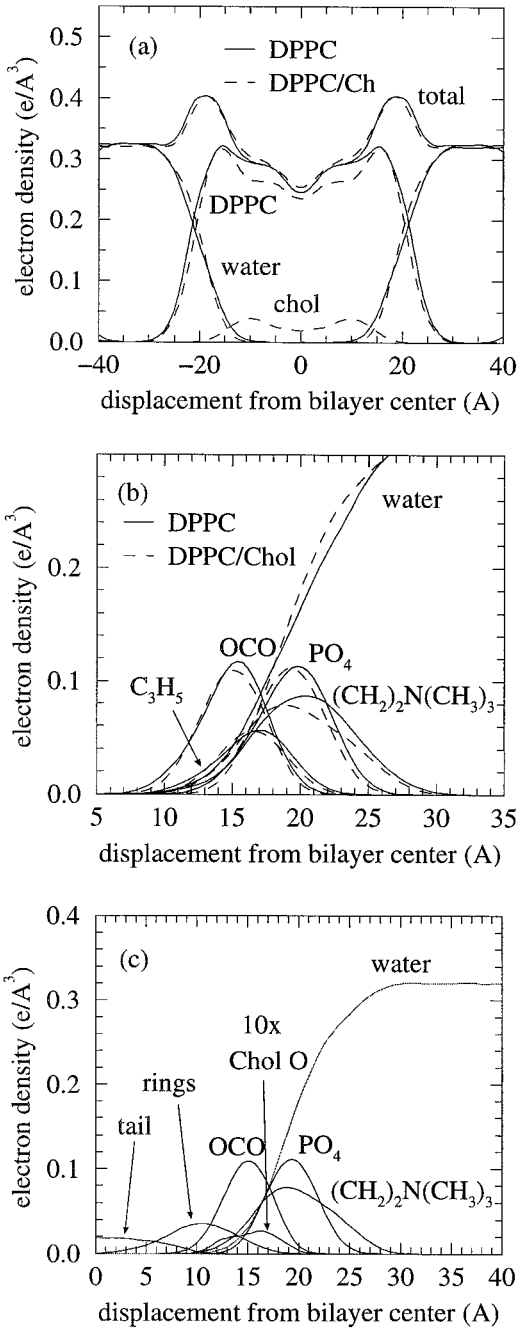

FIGURE 3 (*a*) Symmetrized electron density profiles computed from the simulations with (– – –) and without (——) cholesterol: total electron density profiles and individual contributions from the DPPC, cholesterol, and water molecules. (*b*) Electron density profiles for various groups in the bilayer water interface from simulations with (– – –) and without (——) cholesterol. (*c*) Electron density profiles showing the location of cholesterol in the bilayer/water interfacial region.

of the total electron density profiles, well known from x-ray diffraction studies on L_α phase bilayers (Nagle et al., 1996), consists of two pronounced peaks corresponding roughly to the phosphate groups, a "methyl trough" at the bilayer center, and a region of monotonically decreasing density connecting the peaks and trough. The breakdown into contributions from DPPC and cholesterol shows that the cholesterol molecules remain confined well within the boundaries of the bilayer. Although the total density profiles are similar for the bilayers with and without cholesterol, there are three notable differences. First, the addition of cholesterol decreases the bilayer thickness, as measured by the peak-to-peak distance, from 38.2 ± 0.8 Å to 37.2 ± 0.8 Å (uncertainties are standard deviations of averages from seven 100-ps increments). Second, the total electron density is slightly increased throughout the range where cholesterol exists in the bilayer. Third, the bilayer/water interface is slightly more abrupt, i.e., the DPPC and water densities drop off more abruptly at the edge of the membrane, in the cholesterol-containing bilayer.

To characterize the bilayer/water interface in more detail, following Wiener and White (1992), in Fig. 3 *b* we have broken down the electron densities into contributions from the acyl ester (OC═O), glycerol backbone (C_{3H5}), phosphate (PO_4), and choline ($(CH_2)_2N(CH_3)_3$) groups. With the exception of the choline profiles, the constituent densities are very similar in the DPPC and DPPC/cholesterol bilayers. The peaks in the densities from the cholesterol-containing bilayer have been shifted slightly toward the bilayer center, consistent with the decreased bilayer thickness noted above. The choline density, which is roughly symmetrical in the pure DPPC bilayer, has been skewed significantly toward the center of the cholesterol-containing bilayer so that its peak is concident with the phosphate peak. The narrowing of the bilayer and flattening of the choline group are quantitatively reflected in the average distances of various carbons from the bilayer center along the bilayer normal. For the choline methyl carbons, C_γ (nomenclature according to Büldt et al., 1979); the choline methylene carbons, C_α and C_β; and the glycerol methylene carbon, GC-3, the distances in the pure bilayer are 21.1 ± 3.0 Å, 20.3 ± 2.6 Å, 20.2 ± 2.4 Å, and 17.4 ± 2.1 Å, respectively, compared to the corresponding values in the cholesterol-containing bilayer, 19.8 ± 3.7 Å, 19.6 ± 2.9 Å, 19.6 ± 2.6 Å, and 17.3 ± 2.0 Å. Thus it is clear that the presence of cholesterol causes the choline group to move inward (toward the bilayer center), and the near coincidence of the C_γ, C_α, and C_β distances suggests that the choline group lies nearly flat in the bilayer plane in the cholesterol-containing bilayer. Indeed, the average inclination of the P-N vector is 6° with cholesterol, compared to 17° in the pure DPPC bilayer.

To establish the location of cholesterol in the bilayer, we show in Fig. 3 *c* the electron density contributions from the cholesterol hydroxyl oxygen and ring and tail carbons, along with those from the water and DPPC polar groups. The cholesterol profiles are quite broad, e.g., the hydroxyl oxygen profile has a full width at half-maximum of ~7 Å, indicating a wide range of cholesterol depths in the bilayer. It is clear from the figure that the cholesterol molecules prefer to have their hydroxyl oxygens below the DPPC phosphate groups. Thus cholesterol sits low in the bilayer and leaves holes in the bilayer surface that are generally filled by choline ammonium groups from neighboring

DPPC molecules (hence the nearly flat average orientation of the P-N vectors). The cholesterol hydroxyl position is widely distributed throughout the range where the DPPC ester, phosphate, and choline, as well as the water densities, overlap. In this way, the cholesterol hydroxyl is poised to interact with all of the polar groups in the bilayer/water interface. Indeed, we find that cholesterol does not strongly prefer to interact with a specific DPPC moiety (e.g., acyl ester carbonyl), in agreement with the findings of others (McMullen and McElhaney, 1996). In Fig. 4 we show examples of the types of cholesterol/DPPC and cholesterol/water interactions typically observed in the simulation. A statistical analysis based on radial distribution functions revealed that the hydroxyl group interacts exclusively with water about half of the time, whereas the other half of the time it is equally split between the phosphate and carbonyl groups. Among the interactions with the carbonyl groups, those with the *sn*-1 carbonyl are about twice as common as those with the *sn*-2. The cholesterol ring system is situated such that, on average, C3 (to which the hydroxyl is attached) is at the same distance from the bilayer center (14 Å) as C2 in the DPPC acyl chains, and C17, to which the tail is attached, is at the same distance (7 Å) as C10 in the DPPC chains. The average distances of the DPPC acyl chain carbons are essentially unchanged by the presence of cholesterol compared to their positions in the pure bilayer (Tu et al., 1995b).

From the above analysis of the bilayer/water interfacial region, it is evident that cholesterol modifies the orientation of the choline such that the bilayer surface is flatter. We now examine how this modification affects the orientation of the water molecules and the electrical properties of the bilayer/water interface. Measurements of the electrostatic potential difference across the interface have suggested, and MD simulations have shown, that water molecules in the vicinity of the bilayer surface are preferentially oriented, or "orientationally polarized," such that their dipole vectors (pointing from the oxygen toward the H-H bisector) are directed toward the bilayer surface. Following numerous other authors (reviewed by Feller et al., 1996, and Tobias et al., 1997a), we characterize the water orientational polarization in our simulations by examining the quantity $-\langle\cos\theta\rangle$, where θ is the angle between the water dipole and the bilayer normal, and the brackets denote an average over time, water molecules, and the two bilayer surfaces, as a function of distance from the bilayer center. Clearly, this quantity vanishes for a uniform orientational distribution. The results obtained from our simulations of the pure and cholesterol-containing DPPC bilayers, shown in Fig. 5, display the generic features noted in other simulations. Specifically, there is a peak at roughly the same distance as the maximum in the overall electron density profile (Fig. 3 *a*), which corresponds, as we have already pointed out, to the hydrated DPPC phosphate group and an exponential decay into the bulk water. (We note that at distances less than ~18 Å there are few water molecules and hence the statistics are relatively poor.) We have observed previously that the most specific water/headgroup interactions are those involving the unesterified phosphate oxygens (Tu et al., 1996). As these oxygens are generally pointing into the solution, and the water dipoles tend to point toward these oxygens, the water molecules bound to the phosphate presumably provide the greatest contribution to the orientational polariza-

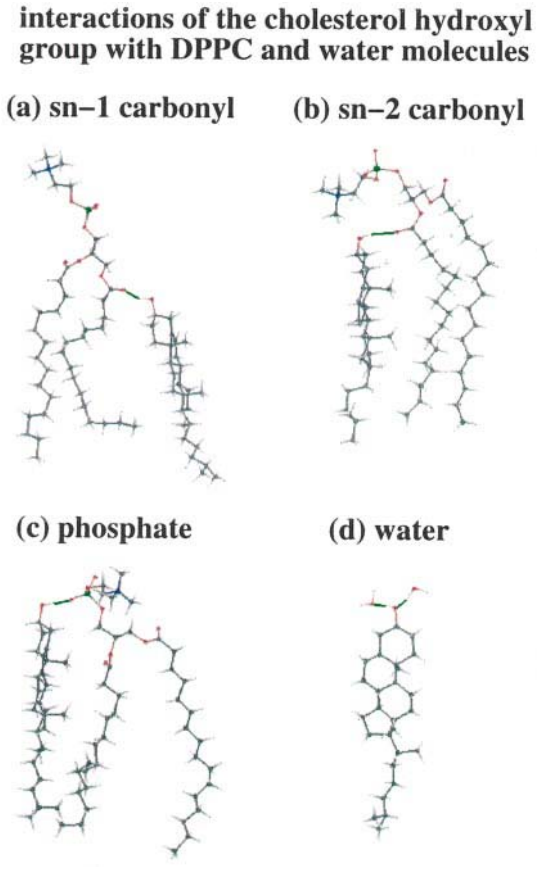

FIGURE 4 Examples of interactions between the cholesterol hydroxyl group and DPPC and/or water molecules. Hydrogen bonds are indicated by green lines.

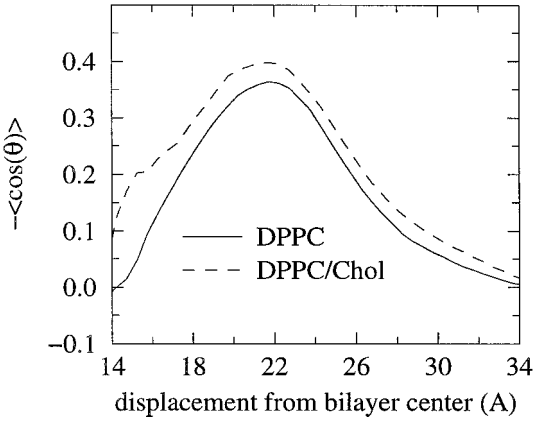

FIGURE 5 Water dipole orientational polarization computed from the simulations with (– – –) and without (——) cholesterol.

tion. Comparing the two profiles, we see that the addition of cholesterol to the bilayer leads to greater orientational polarization of the water molecules throughout the system.

It has long been known from monolayer and bilayer studies that there is an appreciable electric potential difference across lipid/water interfaces (Flewelling and Hubbell, 1986), typically a few hundred mV, negative on the water side relative to air or hydrocarbon in the case of bilayers. Thus the potential can be thought of as arising from an array of dipoles arranged in a plane at the interface. The molecular origins of this so-called dipole potential have been of interest because the electrical properties of the bilayer surface influence the transport of charged species across the membrane. For bilayers composed of diacylphospholipids, the primary negative contributions are from oriented water molecules (Gawrisch et al., 1992) and, to a lesser extent, the carbonyl groups in the acyl ester linkages (Flewelling and Hubbell, 1986). Reports of experimentally measured values of the dipole potential range from −200 mV to −500 mV, depending on the system and type of measurement. Measurements on egg PC/cholesterol monolayers showed that the magnitude of the dipole potential is increased from 415 mV in pure egg PC to 446 mV upon the addition of 0.2 mol% cholesterol (McIntosh et al., 1989). In Fig. 6 *a* we show results for the total dipole potential, calculated from our simulations in the usual way, as a double integral of the charge density (for example, as described by Feller et al., 1996). The average charge density was computed by distributing each partial atomic charge in a Gaussian with a variance equal to the van der Waals radius. Given the crude representation of the molecular charge distributions, and the neglect of explicit electronic polarization in our calculations, we shall use the results solely to draw qualitative conclusions regarding the molecular origins of the dipole potential and its modification by cholesterol. The potentials in Fig. 6 *a* display a monotonic decrease through the bilayer/water interface to a value in the bulk water of about −500 mV for pure DPPC and −800 mV for DPPC, with cholesterol at 12.5 mol%. These results are qualitatively consistent with experimental measurements, although the calculated cholesterol effect is likely too large. To gain insight into the cholesterol effect on the dipole potential, in Fig. 6 *b* we have decomposed the potentials into contributions from the DPPC and water molecules. The potential arising from the DPPC molecules in the pure bilayer suggests that, although there is a negative contribution in the region of the phosphate groups (see Fig. 3 *b*), this is cancelled by the positively charged choline at the outer reaches of the bilayer. Thus, according to our calculations, the dipole potential in the pure bilayer arises primarily because of an excess of water molecules oriented with their dipoles pointing toward the membrane surface. The addition of cholesterol produces an overall negative contribution of more than 100 mV from the DPPC molecules, as well as a ~150-mV increase in the magnitude of the water contribution. The former can be explained in terms of the reduced inclination of the P-N vector leading to incomplete cancellation by the choline of the phosphate dipole, and the latter by an increase in ordered water molecules (indicated above by the orientational polarization) in the cholesterol-containing system. These results constitute a concrete example of the anticipated connection between subtle structural changes and nontrivial modification of the electrical properties of the bilayer surface (Gawrisch et al., 1992).

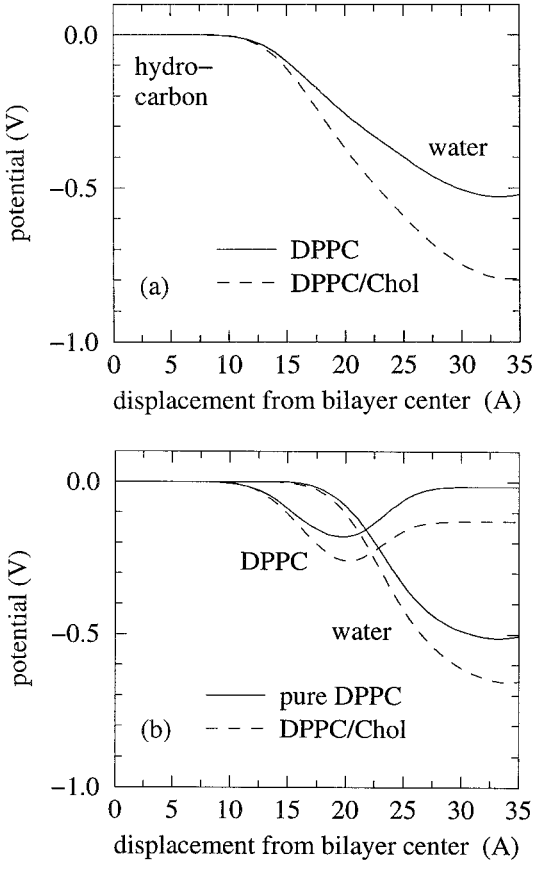

FIGURE 6 Electrostatic potential difference relative to the bilayer center computed from the simulations with (– – –) and without (——) cholesterol. (*a*) Total. (*b*) Individual contributions from water and DPPC molecules.

Now we turn to the bilayer interior and present results concerning the effects of cholesterol on the conformations and packing of the acyl chains. The average hydrocarbon chain structure is often discussed in terms of the C-D order parameter, $S_{CD} = \frac{1}{2}\langle 3\cos^2\theta - 1\rangle$, where θ is the angle between a C-D bond in a deuterated methylene group and the bilayer normal, and the brackets denote an average over time and chains. The order parameter so defined is proportional to the quadrupolar splitting measured in deuterium NMR experiments on deuterated lipids. In Fig. 7 we show the values of S_{CD} calculated from our simulations for each of the methylene groups in the DPPC acyl chains. In a previous publication (Tu et al., 1995b) we compared the results for the pure DPPC bilayer to those measured by deuterium NMR on selectively deuterated lipids (Seelig and Seelig, 1974). The experimental results are notoriously difficult to reproduce quantitatively by MD simulation, and we

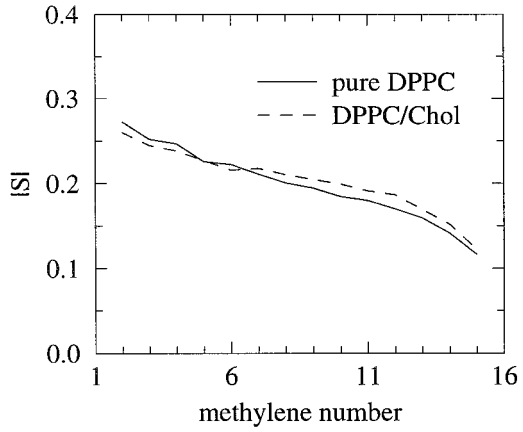

FIGURE 7 Comparison of the DPPC acyl chain C-D order parameters computed from the simulations with (– – –) and without (——) cholesterol.

found that our simulation model, despite giving the correct bilayer dimensions and density, produced too much order at the two extremes of the chains. It is well known from NMR measurements that higher cholesterol concentrations than the one considered here (e.g., >20 mol%) significantly increase S_{CD} values in liquid crystal phase phospholipid bilayers, but at ~10 mol% there is only a slight increase for DMPC (Jacobs and Oldfield, 1979) and DPPC (Vist and Davis, 1990). The simulation results shown in Fig. 7 predict that cholesterol at 12.5 mol% has very little effect on the chain structure as reflected by the S_{CD} values. We arrive at the same conclusion based on the conformational defects: the average fraction of *gauche* conformations in the 14 bonds of the DPPC acyl chains is 25% in both simulations, the distributions of *gauche* conformers along the chains are almost identical (the values for the pure bilayer were reported by Tu et al., 1995b), and there are on average 0.6 *gtg* kinks per chain in both simulations.

Another cholesterol effect that we may address using our simulations is the "condensing" effect, i.e., the tendency of cholesterol to reduce the area or volume per lipid in bilayers. In systems consisting of mixtures of flexible molecules, it is difficult to directly calculate the area and/or volume per molecule, although a potentially useful method for calculating lipid volumes based on density profiles from simulations was reported recently by Petrache et al. (1997). Here we take a simpler approach to qualitatively assess the condensing effect. The average volume of the methylene groups can be estimated from the methylene region of the electron density profiles (Fig. 3 *a*). For example, from the profile for the pure DPPC bilayer, the average electron density in the middle of the acyl chains (distances 6–11 Å from the bilayer center, approximately the range of the fifth through ninth carbons in the chains) is 0.293 $e/Å^3$, which corresponds to a volume 27.3 $Å^3$ per methylene group. For the cholesterol containing bilayer, the average electron density is 0.301 $e/Å^3$, which gives a methylene volume of 26.6 $Å^3$. For perspective, we may compare these results to the corresponding quantities from our previous simulation of a pure gel phase DPPC bilayer. In the gel phase the average methylene electron density and methylene volumes are 0.335 $e/Å^3$ and 23.9 $Å^3$, respectively. Thus, compared to methylene volume change associated with the bilayer phase transition (~10%), the reduction upon addition of 12.5 mol% cholesterol is small (~2%). Given that the average distances of the methylene groups along the bilayer normal are essentially identical in the pure DPPC and DPPC/cholesterol bilayers, we may also conclude that the area per methylene group is not significantly changed by 12.5 mol% cholesterol.

To complement the analysis of the methylene volume, we have calculated the free volume fractions as functions of displacement along the bilayer normal. The free volume properties of bilayers are useful for understanding the passive permeation process (Marrink and Berendsen, 1994). In particular, the profile of the static average free volume fraction provides information on the solubility of penetrants, in the sense of their ability to fit into the various regions of the membrane. We have computed the "empty" free volume fraction as a function of position in the bilayer, exactly as described by Marrink et al. (1996). In Fig. 8 we show the results for our all-atom DPPC and DPPC/cholesterol bilayers at 50°C. For reference we have also indicated the value (0.41) obtained from a simulation of liquid tetradecane that employed the same hydrocarbon chain model at the same temperature (Tobias et al., 1997b). The profiles display some of the general features noted previously by Marrink et al. (1996): they are clearly inhomogeneous throughout the entire bilayer (roughly −20 Å to 20 Å), with maxima at the bilayer center. However, the profile from the DPPC bilayer simulation of Marrink et al. displayed minima in the headgroup region, whereas the minima in our pure DPPC profile appear in the middle of the acyl chain region. Evidently, the shapes of the free volume profiles have a significant model dependence. The results of Marrink et al. were obtained from a simulation employing an "extended

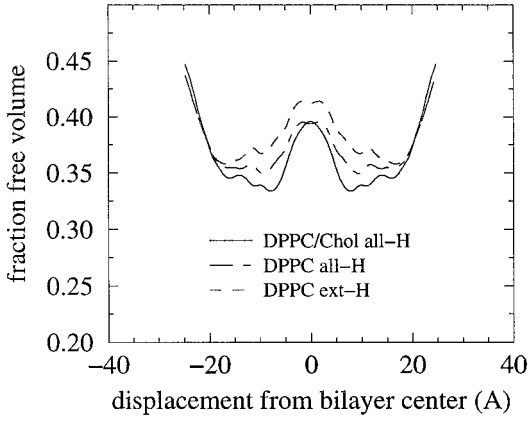

FIGURE 8 Fraction empty free volume as a function of position along the bilayer normal computed using an all-atom model in the bilayers with (——) and without (–·–) cholesterol, and an extended hydrogen model in the bilayer without cholesterol. For reference, the average value calculated from a simulation of tetradecane (Tobias et al., 1997b) is 0.41.

hydrogen" model (methylene and methyl groups represented as single spheres), whereas our simulations included all of the hydrogens. When we recomputed the profile from our DPPC trajectory using an extended-H model for the hydrocarbon chains, we obtained a result that is qualitatively much more similar to that of Marrink et al. (see Fig. 8). Returning to our all-atom results, within the bilayers the empty free volume is everywhere significantly lower than the liquid hydrocarbon reference value. Comparing the DPPC and DPPC/cholesterol profiles, we find that 12.5 mol% cholesterol does reduce the free volume throughout the bilayer, but not by a large amount (the largest reduction is ~4% near the middles of the hydrocarbon chains). Thus we suggest that the cholesterol-induced reduction of bilayer passive permeabilities (e.g., by a factor of 3.5 for acetic acid upon the addition of 20% cholesterol in DPPC at 50°C; Xiang and Anderson, 1997) does not result exclusively from a "condensation" or repacking of the chains such that the steric exclusion of a permeating solute is much greater in a bilayer containing cholesterol at the concentration studied here. Below we will offer an additional explanation based on an analysis of cholesterol effects on molecular dynamics in bilayers.

On the ps to ns time scales, lipid molecules in bilayers exhibit a variety of whole-molecule and internal motions with amplitudes up to ~10 Å that are likely important in the lateral and transbilayer transport of small molecules (König and Sackmann, 1996). For the purpose of qualitatively discussing lipid dynamics in pure and cholesterol-containing bilayers, we show in Fig. 9 sets of configurations spanning three decades of time scales, from 10 ps to 1000 ps, in our MD simulations. As we have pointed out previously (Tobias et al., 1997a), consistent with deductions from incoherent quasielastic neutron scattering (König and Sackmann, 1996), several dynamical processes are developed on the nanosecond time scale in phospholipid bilayers: headgroup "flip-flop," chain defect motion throughout the lengths of the acyl chains, partial rotation of the molecule as a whole, and single-molecule protrusion and lateral "rattling in a cage" motions with amplitudes of several Å. It is clear from the figure that the simulations predict that cholesterol at 12.5 mol% has a profound effect on the phospholipid dynamics at all time scales up to a nanosecond. The nanosecond time scale dynamics in the presence of cholesterol for the most part resemble those on the 100-ps time scale in the pure bilayer, perhaps with the exception of the motions of individual segments of the hydrocarbon chains. It is also of interest to note how, in the example shown in the figure, the arrangement of the *sn*-2 chain is influenced by the methyl groups sticking out of the cholesterol ring system. The amplitudes of the cholesterol protrusion and lateral rattling motions are similar to those of the DPPC molecules. At the bottom of the figure we can see that the cholesterol molecules display a rocking motion (about an axis parallel to the plane of the bilayer, located roughly at the middle of the ring system) around their average, tilted orientation and

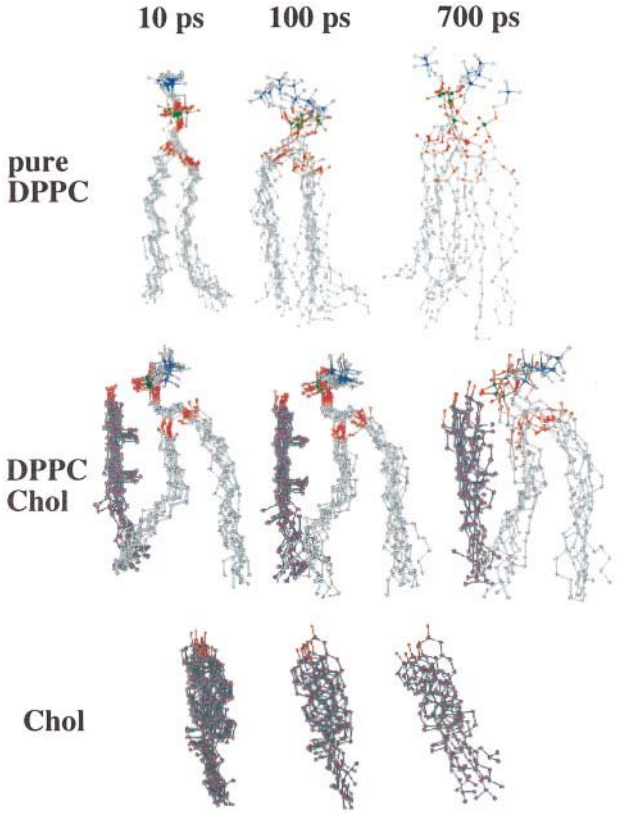

FIGURE 9 Sets of configurations spanning 10-ps, 100-ps, and 700-ps time scales of selected DPPC and cholesterol molecules. The top third of the figure is from the simulation of a pure DPPC bilayer, and the lower two-thirds is from the simulation of the cholesterol containing bilayer.

significant but incomplete rotation of the cholesterol molecules about their long axes on the nanosecond time scale.

The effect of cholesterol on the lateral "rattling" motion of the lipid molecules on the 100-ps time scale is quantitatively illustrated by the time dependence of the center-of-mass mean squared displacements (MSDs) in the bilayer plane plotted in Fig. 10. It is clear that the diffusive motion

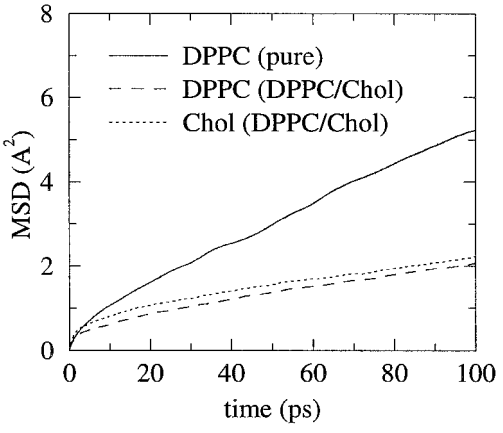

FIGURE 10 Center-of-mass mean squared displacements of DPPC and cholesterol molecules in the bilayer plane computed from simulations of pure and cholesterol-containing DPPC bilayers.

(quantified by the slope of the MSD) of both the DPPC and cholesterol molecules in the cholesterol-containing bilayer is roughly one-third that of the DPPC molecules in the pure bilayer.

The internal dynamics of the hydrocarbon chains, or "fluidity" of the bilayer interior, is conveniently discussed in terms of the time correlation functions plotted in Fig. 11, $C(t) = \frac{1}{2}\langle 3[\mu(t) \cdot \mu(0)]^2 - 1\rangle$, where μ is a unit vector along a methylene C-H bond. As discussed by Venable et al. (1993), these correlation functions generally consist of fast ($<$100 ps) and slow ($>$1 ns) components. It is possible, given an analytical model (typically a sum of exponentials) and either a long ($\gg$1 ns) simulation or an experimental estimate for the slow decay, to fit the computed $C(t)$ and extract amplitudes and relaxation times for the fast motions (Venable et al., 1993). In the absence of sufficiently long simulations, or experimental data on DPPC/cholesterol bilayers, for reliably fitting the $C(t)$, we simply note here that cholesterol increases the reorientational relaxation times along the lengths of the chains. Thus cholesterol acts to increase the microscopic "viscosity" of the bilayer interior. The reorientational correlation functions, $C(t)$, represent a superposition of all of the chain motions occurring on the 100-ps time scale, including simple *trans-gauche* isomerizations, as well as more complicated rerrangements such as kink formation, disappearance, and diffusion. The snapshots shown in Fig. 9 suggest that, whereas the larger amplitude chain motions are quenched, the simpler *trans-gauche* transitions may not be significantly affected by the presence of cholesterol. Indeed, we find, by calculating the isomerization rates as described by Venable et al. (1993), that they are essentially the same along the lengths of the DPPC chains in the pure and cholesterol-containing bilayers. For example, the rates are 19 ns^{-1} and 15 ns^{-1}, respectively, for the second bond (counting from the acyl ester linkage), 23 ns^{-1} and 22 ns^{-1} for the eighth bond, and 38 ns^{-1} and 37 ns^{-1} for the 13th (last) bond in the DPPC acyl chains.

We have compared a constant-pressure and -temperature molecular dynamics simulation of a DPPC bilayer containing 12.5 mol% cholesterol at 50°C to our previous simulation of a pure DPPC bilayer under the same conditions. We have employed force fields that we have validated in previous work by reproducing important structural parameters such as the area per lipid and bilayer thickness of pure DPPC bilayers (Tu et al. 1995b), and in the present work by obtaining good agreement with the x-ray structures of cholesterol crystals, with constant pressure simulations. Our imposition of constant pressure, as opposed to constant volume, represents an advance over the recent simulation of Robinson et al. (1995), and has enabled us to observe cholesterol-induced changes in the overall bilayer dimensions. Indeed, we found that the lamellar spacing increases by ~2.5 Å, consistent with x-ray diffraction data, and the bilayer thickness decreases by ~1 Å. Assuming an unchanged area per DPPC of 61.8 $Å^2$, we obtain 32.4 $Å^2$ for the average area per cholesterol, a value that is significantly lower than the 38 $Å^2$ imposed by Robinson et al.

Our analysis suggested that, in the bilayer interior, cholesterol at the concentration considered does not significantly affect the conformations and packing of the hydrocarbon chains, and only slightly reduces the empty free volume. The bilayer/water interface was modified by the presence of cholesterol such that the lipid headgroups lay flatter to fill spaces left by the cholesterol molecules. This leads to less compensation by the polar lipid headgroups of the water dipole contribution to the membrane dipole potential and provides a plausible explanation for the experimentally observed increase in the magnitude of the dipole potential by the addition of cholesterol. The cholesterol-induced narrowing of the interface could produce a greater free energy barrier for a passively permeating solute and may partially explain the reduction of passive bilayer permeabilities by cholesterol. Our prediction that the bilayer/water interface is narrower in the cholesterol-containing bilayer is at odds with a conclusion of the simulation study by Gabdoulline et al. (1996), namely, that cholesterol acts as a spacer that allows greater headgroup conformational freedom, as suggested by a broader distribution of P-N orientations. However, this result might be an artifact of the excessively condensed bilayer produced by the simulation protocol employed by Gabdoulline et al.

Our simulations also revealed that cholesterol has a significant influence on the subnanosecond time scale lipid dynamics. In summary, we found that large-scale rearrangements of the DPPC acyl chains and the center-of-mass motion of whole lipids are effectively frozen (at least on the ns time scale) and the C-H reorientational motion is slowed somewhat all along the lengths of the hydrocarbon chains by the addition of 12.5 mol% cholesterol. The freezing of the center-of-mass and large-amplitude chain motions could translate into increased friction (microscopic viscosity) for a passively permeating solute. Thus, although we have not made calculations to directly address why cholesterol decreases the passive permeability of fluid phase bilayers, we

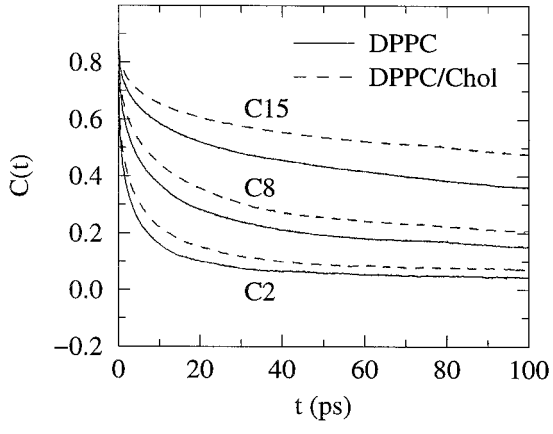

FIGURE 11 Orientational time correlation functions, $C(t) = \langle P_2[\mu(0) \cdot \mu(t)]\rangle$, for selected C-H vectors, μ, in the DPPC acyl chains computed from the simulations with (– – –) and without (——) cholesterol. The numbering of the carbons begins at the carbonyl group of the acyl ester linkage.

speculate that it is affected not only by a tighter interface and reduction in available volume (an energetic effect), but also by an increase in friction (a dynamical effect).

This work was supported in part by grants R01 GM40712 and F32 GM 14463 from the National Institutes of Health. Most of the calculations were performed on the Cray C90 computer at the Pittsburgh Supercomputing Center under Metacenter allocation MCA93S020.

REFERENCES

Allen, M. P., and D. J. Tildesley. 1989. Computer Simulation of Liquids. Oxford University Press, New York.

Berendsen, H. J. C., J. R. Grigera, and T. P. Straatsma. 1987. The missing term in effective pair potentials. *J. Phys. Chem.* 91:6269–6271.

Büldt, G., H. U. Gally, J. Seelig, and G. Zaccai. 1979. Neutron diffraction studies on phosphatidylcholine model membranes. I. Head group conformation. *J. Mol. Biol.* 134:673–691.

Carruthers, A., and D. L. Melchior. 1983. Studies of the relationship between bilayer water permeability and physical state. *Biochemistry.* 22:5797–5807.

Craven, B. M. 1979. Pseudosymmetry in cholesterol monohydrate. *Acta Crystallogr. B.* 35:1123–1128.

Feller, S. E., R. W. Pastor, A. Rojnuckarin, S. Bogusz, and B. R. Brooks. 1996. Effect of electrostatic force truncation on interfacial and transport properties of water. *J. Phys. Chem.* 100:1701–17020.

Flewelling, R. F., and W. L. Hubbell. 1986. The membrane dipole potential in a total membrane potential model. *Biophys. J.* 49:541–552.

Gabdoulline, R. R., G. Vanderkooi, and C. Zheng. 1996. Comparison of the structures of dimyristoylphosphatidylcholine in the presence and absence of cholesterol by molecular dynamics simulations. *J. Phys. Chem.* 96:15942–15946.

Gawrisch, K. D., D. Ruston, J. Zimmerberg, V. A. Parsegian, R. P. Rand, and N. Fuller. 1992. Membrane dipole potentials, hydration forces, and the ordering of water at membrane surfaces. *Biophys. J.* 61:1213–1223.

Hui, S. W., and N.-B. He. 1983. Molecular organization in cholesterol-lecithin bilayers by x-ray and electron diffraction measurements. *Biochemistry.* 22:1159–1164.

Jacobs, R., and E. Oldfield. 1979. Deuterium nuclear magnetic resonance investigation of dimyristoyllecithin-dipalmitoyllecithin and dimyristoyllecithin-cholesterol mixtures. *Biochemistry.* 18:3280–3285.

Köhnig, S., and E. Sackmann. 1996. Molecular and collective dynamics of lipid bilayers. *Curr. Opin. Colloid Interface Sci.* 1:78–82.

Marrink, S.-J., and H. J. C. Berendsen. 1994. Simulation of water transport through a lipid membrane. *J. Phys. Chem.* 98:4155–4168.

Marrink, S. J., R. M. Sok, and H. J. C. Berendsen. 1996. Free volume properties of a simulated lipid membrane. *J. Chem. Phys.* 104: 9090–9099.

McIntosh, T. J., A. D. Magid, and S. A. Simon. 1989. Cholesterol modifies the short-range repulsive interactions between phosphatidylcholine bilayers. *Biochemistry.* 28:17–25.

McMullen, T. P. W., and R. N. McElhaney. 1996. Physical studies of cholesterol-phospholipid interactions. *Curr. Opin. Colloid Interface Sci.* 1:83–90.

Méléard, P., C. Gerbeaud, T. Pott, L. Fernandez-Puente, I. Bivas, M. D. Mitov, J. Dufourcq, and Pierre Bothorel. 1997. Bending elasticities of model membranes: influences of temperature and sterol content. *Biophys. J.* 72:2616–2629.

Nagle, J. F., R. Zhang, S. Tristram-Nagle, W.-J. Sun, H. I. Petrache, and R. M. Suter. 1996. X-ray structure determination of fully hydrated L_α phase dipalmitoylphosphatidylcholine bilayers. *Biophys. J.* 70: 1419–1431.

Oldfield, E., M. Meadows, D. Rice, and R. Jacobs. 1978. Spectroscopic studies of specifically deuterium labeled membrane systems. Nuclear magnetic resonance investigation of the effects of cholesterol in model systems. *Biochemistry.* 17:2727–2740.

Pastor, R. W. 1994. Molecular dynamics and Monte Carlo simulations of lipid bilayers. *Curr. Opin. Struct. Biol.* 4:486–492.

Petrache, H. I., S. E. Feller, and J. F. Nagle. 1997. Determination of component volumes of lipid bilayers from simulations. *Biophys. J.* 72:2237–2242.

Robinson, A. J., W. G. Richards, P. J. Thomas, and M. M. Hann. 1995. Behavior of cholesterol and its effect on head group and chain conformations in lipid bilayers: a molecular dynamics study. *Biophys. J.* 68:164–170.

Rohrer, D. C., W. L. Duax, J. F. Griffin, and C. M. Weeks. 1980. Conformational analysis of sterols: comparison of x-ray crystallographic observations with data from other sources. *Lipids.* 15:783–792.

Seelig, A., and J. Seelig. 1974. Dynamic structure of fatty acyl chains in a phospholipid bilayer measured by DMR. *Biochemistry.* 13:4839–4845.

Shieh, H.-S., L. G. Hoard, and C. E. Nordman. 1981. The structure of cholesterol. *Acta Crystallogr. B.* 37:1538–1543.

Tobias, D. J., K. Tu, and M. L. Klein. 1997a. Atomic-scale molecular dynamics simulations of lipid membranes. *Curr. Opin. Colloid Interface Sci.* 2:15–26.

Tobias, D. J., K. Tu, and M. L. Klein. 1997b. Assessment of all-atom potentials for modeling membranes: molecular dynamics simulations of solid and liquid alkanes and crystals of phospholipid fragments. *J. Chim. Phys. Phys.-Chim. Biol.* 94:1482–1502.

Tu, K. 1995. Molecular dynamics studies of phospholipid bilayers. Doctoral dissertation. University of Pennsylvania.

Tu, K., D. J. Tobias, and M. L. Klein. 1995a. Constant pressure and temperature molecular dynamics simulations of crystals of the lecithin fragments: glycerylphosphorylcholine and dilauroylglycerol. *J. Phys. Chem.* 99:10035–10042.

Tu, K., D. J. Tobias, and M. L. Klein. 1995b. Constant pressure and temperature molecular dynamics simulation of a fully hydrated liquid crystal phase dipalmitoylphosphatidylcholine bilayer. *Biophys. J.* 69: 2558–2562.

Tu, K., D. J. Tobias, and M. L. Klein. 1996. Molecular dynamics investigation of the structure of a fully hydrated gel-phase dipalmitoylphosphatidylcholine bilayer. *Biophys. J.* 70:595–608.

Venable, R. M., Y. Zhang, B. J. Hardy, and R. W. Pastor. 1993. Molecular dynamics simulations of a lipid bilayer and of hexadecane: an investigation of membrane fluidity. *Science.* 262:223–226.

Vist, M. R., and J. H. Davis. 1990. Phase equilibria of cholesterol/dipalmitoylphosphatidylcholine mixtures: ^{2}H nuclear magnetic resonance and differential scanning calorimetry. *Biochemistry.* 29:451–464.

Weber, H.-P., B. M. Craven, P. Sawzik, and R. K. McMullan. 1991. Crystal structure and thermal vibrations of cholesteryl acetate from neutron diffraction at 123 and 20 K. *Acta Crystallogr. B.* 47:116–127.

Wiener, M. C., and S. H. White. 1992. Structure of a fluid dioleoylphosphatidylcholine bilayer determined by joint refinement of x-ray and neutron diffraction data. 3. Complete structure. *Biophys. J.* 61:434–447.

Williams, D. E. 1967. Nonbonded potential parameters derived from crystalline hydrocarbons. *J. Chem. Phys.* 47:4690–4684.

Xiang, T.-X., and B. D. Anderson. 1997. Permeability of acetic acid across gel and liquid-crystalline lipid bilayers conforms to free-surface-area theory. *Biophys. J.* 72:223–237.